Generalizing asymmetric and pseudo-Voigt functions by means of q-Gaussian Tsallis functions to analyze the wings of Raman spectral bands

Generalizing asymmetric and pseudo-Voigt functions by means of q-Gaussian Tsallis functions to analyze the wings of Raman spectral bands

Amelia Carolina Sparavigna

Department of Applied Science and Technology, Polytechnic University of Turin, Italy

Email: amelia.sparavigna@polito.it

Torino, October 19, 2023.

Abstract

It is important, for further applying the q-Gaussian Tsallis functions, to discuss how they can generalize asymmetric and pseudo-Voigtian functions. Some remarks about Voigt functions are also stressed, regarding the behavior of the wings of Raman spectral components. The use of Voigt and pseudo-Voigt functions implies the wings as Lorentzian, but this is not observed for the Raman bands. At the same time, the wings are not Gaussians, and for this reason q-Gaussians are fundamental for evidencing wing behavior.

Keywords: Tsallis q-Gaussian distribution, Asymmetric q-Gaussian distribution, Voigt distribution, pseudo-Voigt distribution

Introduction

q-Gaussian functions, also known as "Tsallis functions", are probability distributions derived from the Tsallis statistics (Tsallis, 1988, 1995, Hanel et al., 2009). The q-Gaussians are based on a generalized form of the exponential function (see discussion in Sparavigna, 2022), characterized by a continuous parameter q in the range $1 < q < 3$. As given by Umarov et al., 2008, the q-Gaussian function is based on function $f(x) = Ce_q(-\beta x^2)$, where $e_q(.)$ is the q-exponential function and C a constant. In the exponent, we use $\beta = 1/(2\sigma^2)$, with variance σ. The q-exponential has expression: $exp_q(u) = [1 + (1-q)u]^{1/(1-q)}$, which possesses a bell-shaped profile. In the case that we have the peak of the function at position x_o, the q-Gaussian is given as:

q-Gaussian = $Cexp_q(-\beta(x-x_o)^2) = C[1-(1-q)\beta(x-x_o)^2]^{1/(1-q)}$

For q equal to 2, the q-Gaussian is the Cauchy-Lorentzian distribution (Naudts, 2009). In Moyano et al., 2006, the researchers stress that the q-Gaussian "recovers the t-Student distribution with *l* degrees of freedom if q = (3 + *l*)/(*1* + l). For *l* = 1, hence q = 2, we get the Cauchy-Lorentz distribution" (see Appendix A for further discussion). For q close to 1, we have the usual Gaussian form.

For the q-parameter between 1 and 2, the shape of the q-Gaussian function is intermediate between the Gaussian and the Lorentzian profile. Its behavior turns the q-Gaussian into a function suitable for the analysis of Raman spectra, because the spectral bands also are characterized by intermediate profiles between Lorentzian and Gaussian outlines (Kirillov, 2004). Besides these two functions, which remain the most popular for fitting Raman spectra, *linear combinations* (pseudo-Voigt distributions) or *convolutions* of them (Voigt distributions) are used too (Meier, 2005). The Voigtian convolution function turns out into a bell shape with a Gaussian kernel and wings which are asymptotically of the Lorentz form (as determined by Cope and Lovett, 1987, the asymptotic solution of Voigtian expansion has the leading term $a_0/\pi x^2$). In some literature, the wings are also mentioned as "tails".

Therefore, as told in Townsend, 2008, the "Voigt function looks like Gaussian for small x (i.e., near line center), and like Lorentzian for large x (i.e., out in line wings)". We can also appreciate this fact by observing the pseudo-Voigt function, which is generally used for approximating the Voigt function. Being the pseudo-Voigt the linear combination of a Gaussian and Lorentzian functions, the wings must be necessarily Lorentzian and the kernel Gaussian-like.

Consequently, if we use Voigt functions or pseudo-Voigt functions, the wings of the Raman bands will be always described by a Lorentzian behavior. It is reasonable to ask ourselves: is this always the experimental case? That is, are we always observing Lorentzian wings for the Raman bands? This is a fundamental question. A generalization of Voigt and pseudo-Voigt functions obtained by means of q-Gaussians can help us in describing the leading term of the band wings, that is, to measure the wings, besides telling whether it is Lorentzian or not. The q-Gaussians are therefore the solution of the question. The same is true for the use of asymmetric q-Gaussians.

Spectroscopy and convolution

In general, regarding the spectroscopy, let us consider the words by Orazio Svelto, 1970, about the homogeneous broadening of the photon emission. In the case that we have a dipole damped oscillator model, we can observe the spectral line of the spontaneous emission with a "natural" or "intrinsic" broadening. This homogeneous broadening produces a line profile described by a Lorentzian function. Orazio Svelto is also mentioning the photon-phonon interaction as generating homogeneous broadening and therefore a Lorentzian line shape too. An inhomogeneous broadening (such as those caused by the Doppler effect and thermal effect) is giving a Gaussian line shape. However, the most observed case is that of an intermediate profile, given by the convolution of the resonance relative probability and the broadening function, because natural band can be modified by different mechanisms (Svelto, 1970).

We have mentioned the natural broadening giving a Lorentzian profile, the thermal broadening introducing a Gaussian profile, and the general intermediate profiles as the most common cases. A consequence is that the Voigt profile, that is the convolution of Gaussian and Lorentzian functions, is used to simulate the intermediate case. "Alternatively, [we can] suppose that the line is scanned by a spectrophotometer with a Gaussian sensitivity function" (Tatum, 2022). Then, in this experimental framework, we have the convolution of the line with the instrumental function profile. Let us remember that "the general expression that takes account of all the instrumentally induced distortion of the true band shape can be called the instrument function" (Seshadri and Jones, 1963). It is also known as the "instrumental transfer function" (Merlen et al., 2017).

As told by S.G. Rautian, 1958: "Each monochromatic component $\varphi(x)dx$ of the true radiation is replaced by the apparatus [instrument] function, as a result of which, at some arbitrary point x', there is created an illumination (or current) $a(x'-x)\varphi(x)dx$. Other monochromatic components of the true distribution also make a corresponding contribution to the illumination at the point x', and as a result the observed distribution $f(x')$ will be expressed by the following integral":

$$f(x') = \int_{-\infty}^{+\infty} a\,(x'-x)\varphi(x)dx.$$

In the integral we have function $a(x)$ that considers "distortions both in the optical and recording parts of the apparatus" (Rautian, 1958). In Rautian, 1958, we can find several different instrumental functions that can be convoluted with the true radiation. And the true radiation can be a convolution of different broadening mechanisms. The Voigt convolution is based on Lorentzian and Gaussian profiles because the analysis starts from a Lorentzian damping model (natural radiation) with a weight which is a Gaussian one. Different approaches exist (Kirillov, 2004), so that the true radiation line can be assumed different from a Lorentzian function; moreover, the weight function can be different from a pure Gaussian function.

In Merlen et al., 2017, researchers are telling that "If we do not take into account the instrumental transfer function that can be negligible in many cases (...), the total intensity of one phonon mode with a wavevector q_0 and a frequency $\omega(q_0)$, in a perfect crystal, is spread on a symmetric profile which is Lorentzian". Between brackets (…), Merlen and coworkers tell that "If the natural width is comparable to the width of the instrumental transfer function, which is generally a Gaussian function, then the intensity of the band is a convolution between the natural line shape and the instrumental function. Depending on the grating used, the instrumental width varies but is in general close to 1 cm^{-1}." An investigation regarding the transfer function is therefore necessary, at least to determine whether its role is negligible or not. The transfer function can be relevant when the decomposition (deconvolution) of the component bands is the aim of the research.

For decomposition (deconvolution) of peaks, laser sources and diffraction gratings are playing a fundamental role (see the discussion in https://www.edinst.com/blog/spectral-resolution-in-raman-spectroscopy/ for instance). "As long as the resolution is greater than the linewidth, the user will get all the information from the Raman spectrometer regardless of whether a high- or low-resolution system is used. … The characterization of polymorphs and crystallinity are two examples of when the user may need the highest possible resolution".

With its intermediate behavior, the q-Gaussian is suitable to describe convolution mechanisms in general. For the spectra previously considered (Sparavigna, 2023), we have shown that q-Gaussians are able of fitting the bands in a successful manner. This is the case of graphite, as shown in ChemRxiv1, of anatase in ChemRxiv2, and also of SERS spectra in ChemRxiv3. But we have also seen that in the far-wing region, in the case of Diamond (SSRN), a linear combination of q-Gaussians can provide the perfect result.

Further spectra need to be analyses, especially for the case of isolated peaks, because here our aim is that of determining the leading term of the wing behavior, to answer the question posed in the Itroduction.

Generalizing pseudo-Voigt and asymmetric functions

Being the Voigt function the convolution of a Gaussian and a Lorentzian function, we could imagine generalizing it by considering the convolution of two q-Gaussians. However, as in the case of the Voigtian functions, a numerical approach is necessary to calculate them. Therefore, we prefer to approach the q-generalization of the pseudo-Voigtian functions, performed in the following manner:

$$\text{q-generalized-P-V} = C_1[1-(1-q_1)\beta_1(x-x'_o)^2]^{1/(1-q_1)} + C_2[1-(1-q_2)\beta_2(x-x''_o)^2]^{1/(1-q_2)}$$

This is a linear combination of q-Gaussian functions. We consider the possibility to allow a slight difference of the centers of the two q-Gaussians, imagining including a small asymmetry of the Raman band. Being the Lorentzian function a q-Gaussian with q=2, and being the Gaussian function numerically indistinguishable from the q-Gaussian with q=1.01, the pseudo-Voigt turns out being:

$$\text{P-V} = C_1[1-(1-1.01)\beta_1(x-x'_o)^2]^{1/(1-1.01)} + C_2[1-(1-2.0)\beta_2(x-x''_o)^2]^{1/(1-2.0)}$$

We use a q-Gaussian with q=1.01 instead of a Gaussian, because these two functions are numerically indistinguishable.

Raman bands can be asymmetric and q-Gaussians can be relevant also in this case (ChemRxiv4). In the discussion in ChemRxiv4, we proposed the q-BWF functions, but here we consider the asymmetric Tsallis q-Gaussians as given in Devi, 2021, that is:

q-Gaussian_LEFT = $Cexp_{q_L}(-\beta_L(x-x_o)^2) = C[1-(1-q_L)\beta_L(x-x_o)^2]^{1/(1-q_L)}$,

when $x - x_o < 0$

q-Gaussian_RIGHT = $Cexp_{q_R}(-\beta_R(x-x_o)^2) = C[1-(1-q_R)\beta_R(x-x_o)^2]^{1/(1-q_R)}$,

when $x - x_o > 0$

Parameters q and β of the Left and Right parts are different.

To answer our question, that is to understand if we have always Lorentzian wings for Raman components, our approach is that of considering experimental Raman spectra.

Diamond

As previously told, in the case of Diamond (as shown in SSRN) a linear combination of q-Gaussians can provide a perfect result. Here in the following an example. The spectrum is from RRUFF database (Lafuente et al., 2015). Let us start from a single q-Gaussian fit.

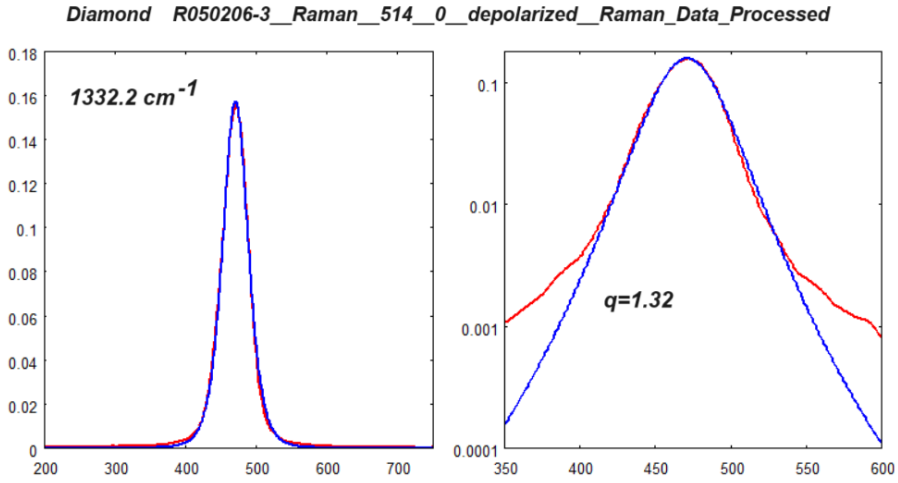

Fig.1: Best fit (blue) onto RRUFF ID R050206 Raman spectrum (red). A q-Gaussian is used (the value of the q-parameter is given in the figure). On the right, the same fit is shown with the log scale for y-axis (semi log scale). Data and q-Gaussian function are given as functions of integers n (equally spaced points), for the x-axis which is representing the Raman shift. A convenient scale is used for the y-axis (intensity axis). The fitting calculation is obtained by minimizing the sum of the squares of deviations (sum on n from 200 to 800 equal to 1.0 x 10^{-3}).

The semi log scale is evidencing that the wings have a behavior different from those of the q-Gaussian giving the best fit. So let us propose to fit the band with the generalized form of the pseudo-Voigt function. The best fit is given in the following figure.

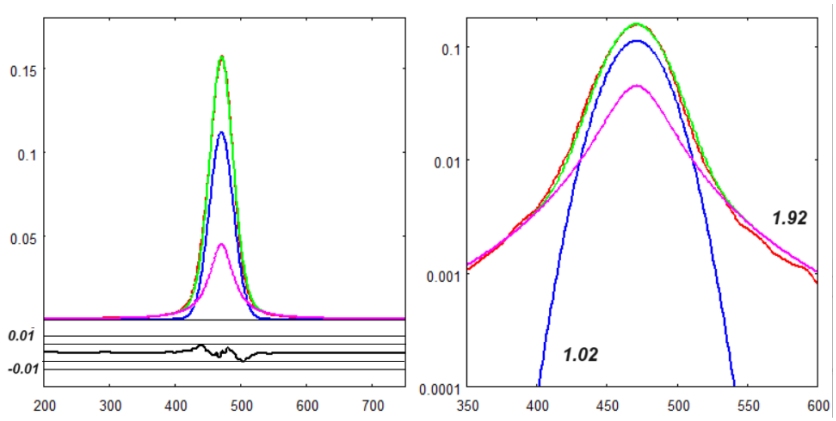

Fig.2: Best fit (green) onto RRUFF ID R050206 Raman spectrum (red). Two q-Gaussians are used (the value of the q-parameters is given in the figure). On the right, the same fit is shown with the log scale for y-axis (semi log scale). The sum of the squares of deviations (sum from n=200 to n=800) is equal to 7.1 x 10^{-4}.

We can see from the Fig.2, that we have a slight asymmetry and that far-wing behavior is not Lorentzian. The leading term has a power equal to -1.087 . Let us use one asymmetric q-Gaussian: the result is given in the Fig.3.

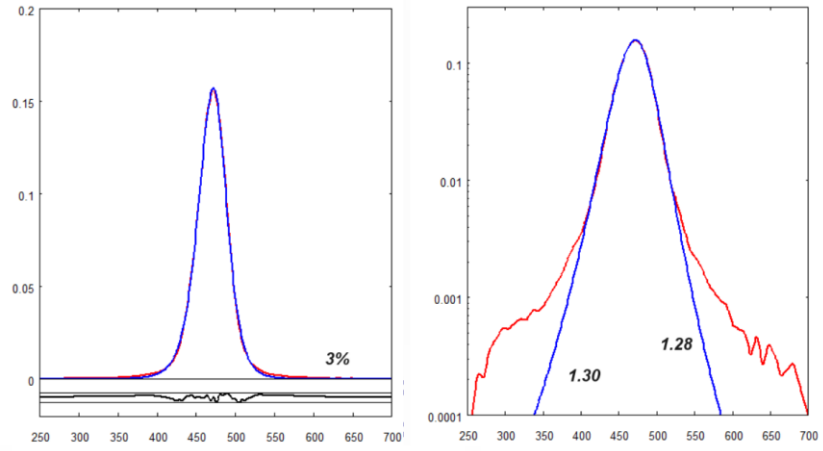

Fig.3: Best fit with an asymmetric q-Gaussian. The q-parameters of Left and Right parts are given in the right panel. The lower part of figure on the left is giving the misfit. The misfit band is large 0.005. The ratio of this misfit band width and the height of the peak is 3%. The fitting calculation is obtained by minimizing the sum of the squares of the deviations (sum from n=200 to n=800 equal to 3.4 x 10^{-4}).

In the lower part of the Figure 3 on the left, we can also appreciate the misfit. The misfit band is large 0.005, in the arbitrary units of the y-axis used for the plot. The ratio of this misfit band width and the height of the peak is 3%. The result is very good indeed, and also in this case which is the "worst case" for q-Gaussians among those proposed in SSRN. It is evident that the fit is regarding all the Raman band, and not only the center of if or its far wings.

Let us consider again the Figure 2, where we have a best fit with two q-Gaussians. Here the ratio between misfit band width and the height of the peak is of 6%. This means that asymmetry exists and

that the comparison to asymmetric q-Gaussians is relevant. In any case, could we do better with a pseudo-Voigt function? The answer is no for sure because the pseudo-Voigt function is a special case of the q-Gaussian generalization.

For what is regarding the fitting procedure, for comparing q-Gaussians and pseudo-Voigtians it must be the same. For comparison with a Voigt function, we must consider a further intrinsic difficulty, besides that related to the fitting procedure. When we use a Voigt function, we necessarily need a numerical approximation of the convolution and consequently we can obtain different results by changing this approximation. In literature, it is generally told that Voigt functions are used for fitting, but no details are provided about the calculation of them.

Let us continue investigating other spectra.

Barite, Celestine and Anglesite

Barite or baryte is a mineral consisting of barium sulfate ($BaSO_4$). "The baryte group consists of barite, celestine (strontium sulfate), anglesite (lead sulfate), and anhydrite (calcium sulfate). Baryte and celestine form a solid solution $(Ba,Sr)SO_4$" (Wikipedia mentioning Hanor, 2000).

Let us consider spectrum https://rruff.info/Barite/R040036 .

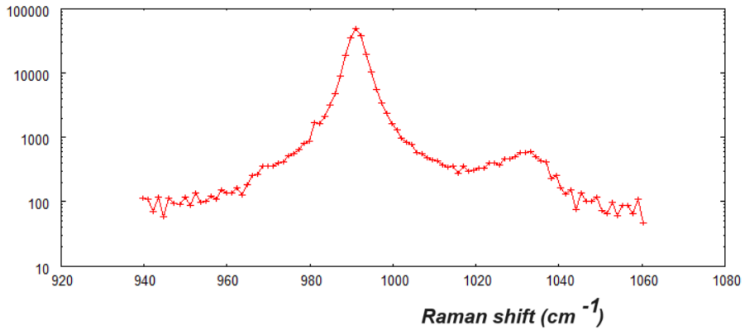

Fig.4: The plot shows the spectrum RRUFF ID R040036 near the main peak at 991 cm^{-1} in semi log scale. To fit the peak, we consider a narrow interval of Raman shift to avoid the need of a further component.

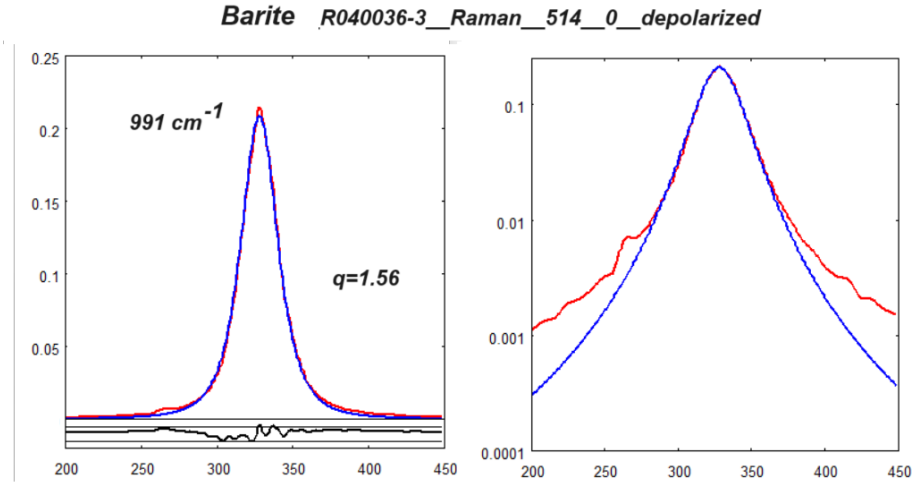

Fig.5: Best fit (blue) onto RRUFF ID R040036 Raman spectrum (red). A q-Gaussian is used (the value of the q-parameter is given in the figure). The misfit is proposed in the lower part of the plot (the misfit band is large 0.01). On the right, the same fit is shown with the log scale for y-axis (semi

log scale). Data and q-Gaussian function are given as functions of integers n (equally spaced points), for the x-axis which is representing the Raman shift. A convenient scale is used for the y-axis (intensity axis). The fitting calculation is obtained by minimizing the sum of the squares of the deviations (sum from n=200 to n=450 equal to 1.2 x 10^{-3}).

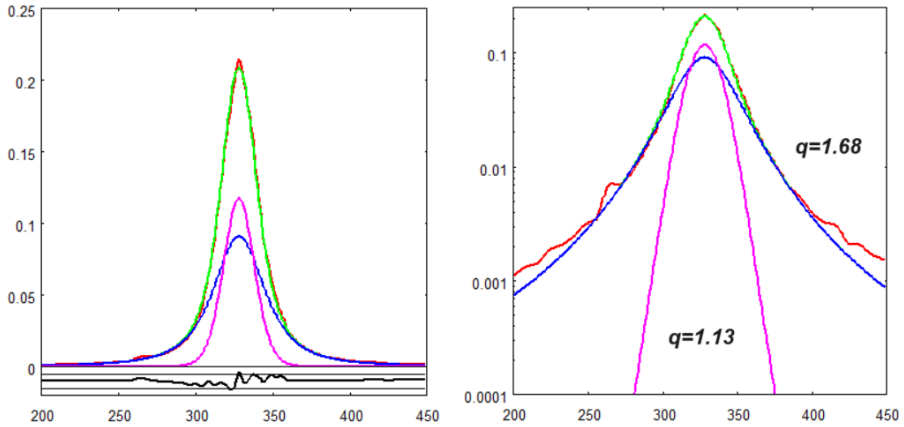

Fig.6: Best fit (green) onto RRUFF ID R040036 Raman spectrum (red). Two q-Gaussians to generalize the pseudo-Voigt functions are used (the values of the q-parameters are given in the figure). The fitting calculation is obtained by minimizing the sum of the squares of the deviations (sum from n=200 to n=450 equal to 6.9 x 10^{-4}). The misfit band is 0.01 large.

It is also relevant to consider an asymmetric q-Gaussian fit.

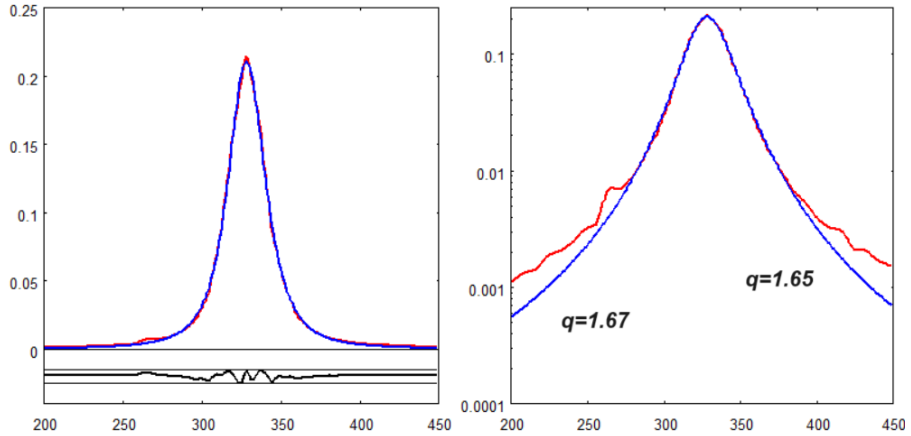

Fig.7: Best fit (blue) onto RRUFF ID R040036 Raman spectrum (red). An asymmetric q-Gaussian is used (the values of the q-parameters, left and right, are given in the figure). The fitting calculation is obtained by minimizing the sum of the squares of deviations (sum from n=200 to n=450 equal to 5.5 x 10^{-4}). The misfit band is 0.01 large.

For barite R040036, it is the asymmetric q-Gaussian to provide the smaller the sum of the squares of deviations.

In the caption of Fig.4 it told that to avoid the need of a further component we use a narrow interval of the Raman shift. For the case of the asymmetric q-Gaussian, let us consider all the range given in the Fig.4, the result of the fit is given in the following: the fit does not change in the value of q-parameters.

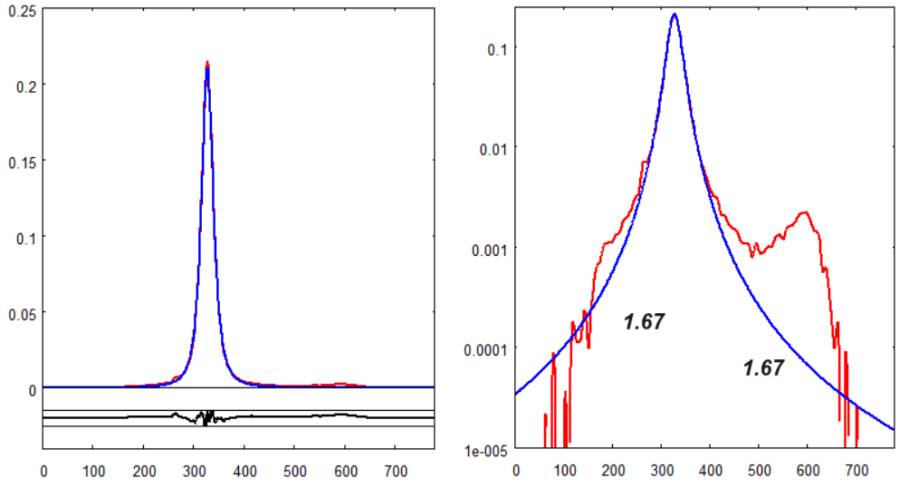

Fig.8: Best fit (blue) onto RRUFF ID R040036 Raman spectrum (red). An asymmetric q-Gaussian is used. The fitting calculation is obtained by minimizing the sum of the squares of the deviations (sum from n=1 to n=780 equal to 8.6 x 10^{-4}). The misfit band is 0.01 large.

Let us pass to Celestine, https://rruff.info/celestine/display=default/R040007 .

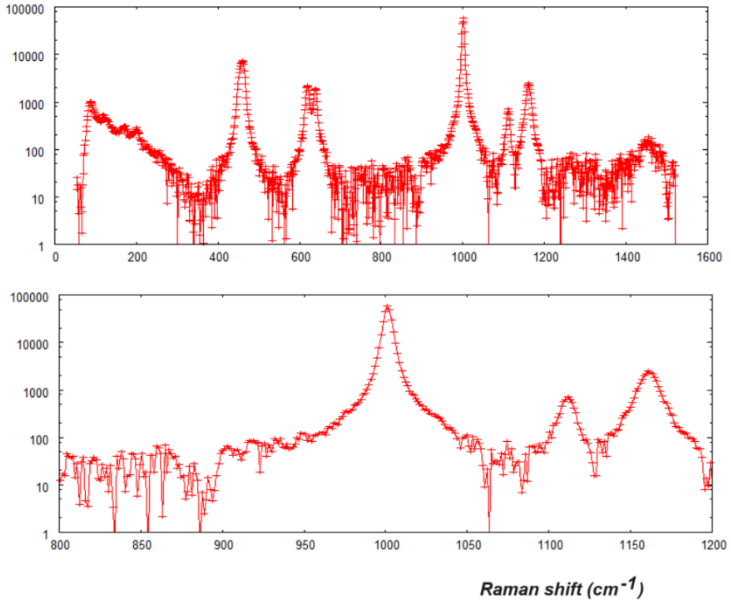

Fig.9: RRUFF ID R040007 Raman spectrum (0° depolarized) in the upper part and a detail of it in the lower part, both in semi log scale.

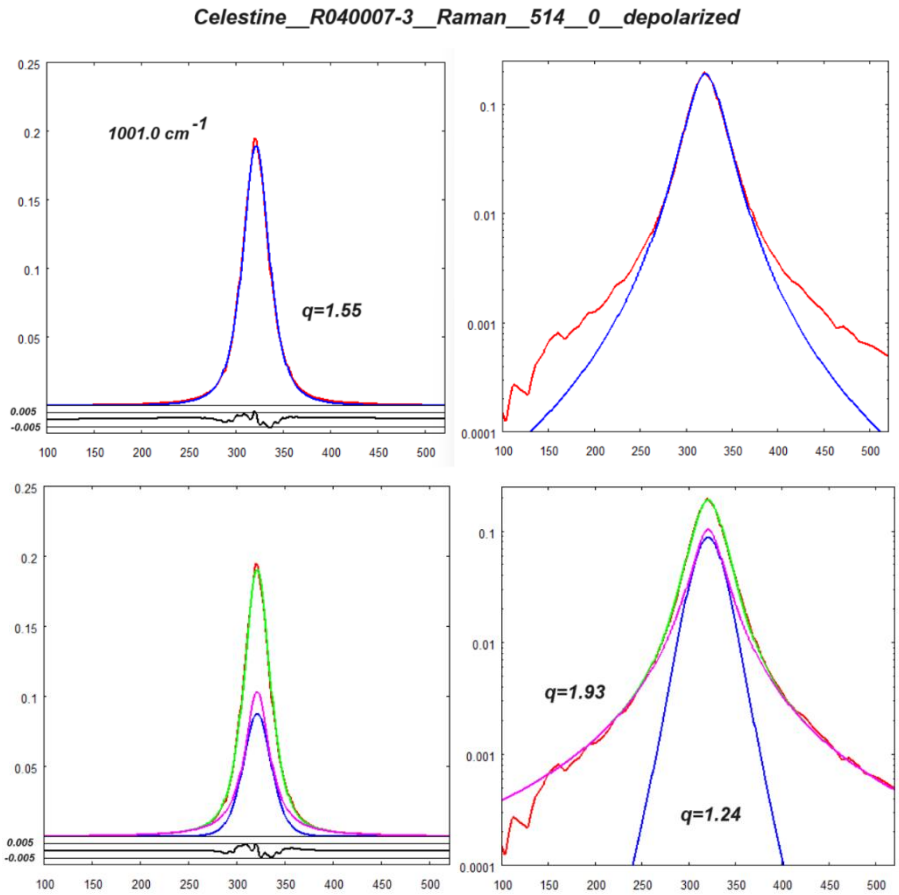

Fig.10: Upper part: best fit (blue) onto RRUFF ID R040007 Raman spectrum (red), when a q-Gaussian is used. In the lower part the best fit is in green, and two q-Gaussians are used. The minimized sums of the squares of the deviations are equal to 8.0 x 10^{-4} and 5.7 x 10^{-4}, respectively (sums from 100 to 510).

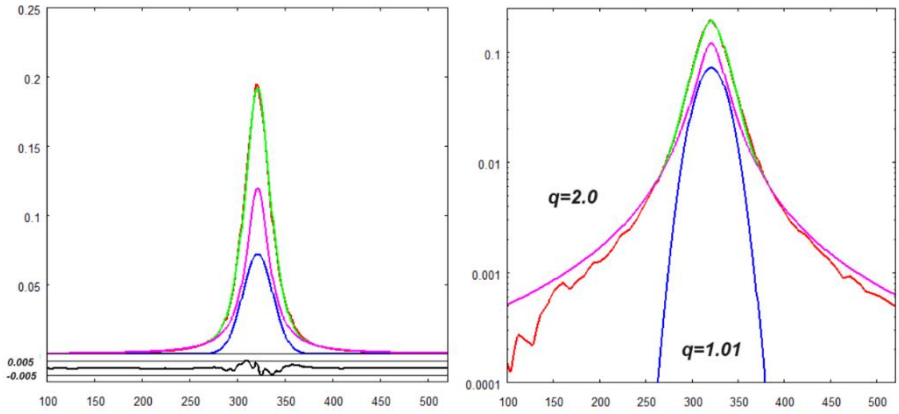

Fig.11a: Best fit (green) onto RRUFF ID R040007 Raman spectrum (red), when a Gaussian (q=1.01) and a Lorentzian (q=2.0) are used. The minimized sum of the squares of the deviations is equal 6.5 x 10^{-4} (sums from 100 to 510).

In the Figure 11a the pseudo-Voigt fitting of the Celestine spectrum is given. The sum of the squares of the deviations is larger than that of the fit with two q-Gaussians given in the Figure 10. Let us note that the far-wing behavior is different.

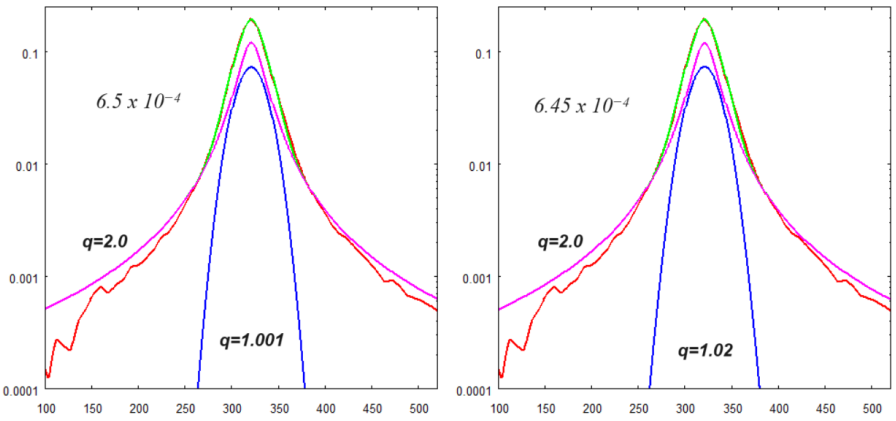

Fig.11b: Best fit (green) onto RRUFF ID R040007 Raman spectrum (red), with q=1.001 on the left and q=1.02 on the right. The minimized sum of the squares of the deviations is equal to 6.5 x 10^{-4} on the left and 6.45 x 10^{-4} on the right.

The choice of q=1.01 for the q-Gaussian as representative of a Gaussian function could be questionable. Therefore, we add the Fig.11b, which is showing the fit with q=1.001 and q=1.02. The minimized sum of the squares of deviations is the same for q=1.01 and q=1.001.

Let us pass to Anglesite, https://rruff.info/Anglesite/R050408 .

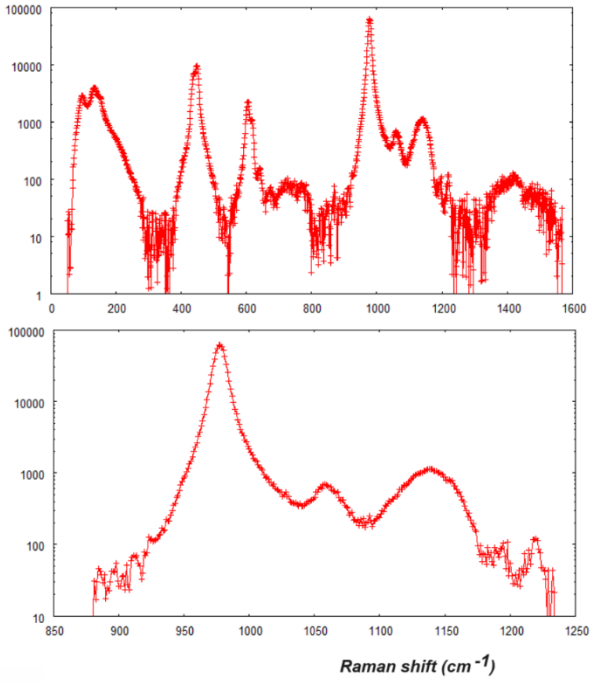

Fig.12: RRUFF ID R050408 Raman spectrum (0° depolarized) in the upper part and a detail of it in the lower part, both in semi log scale.

Here in the following figure, an asymmetric q-Gaussian is used for fitting the main peak.

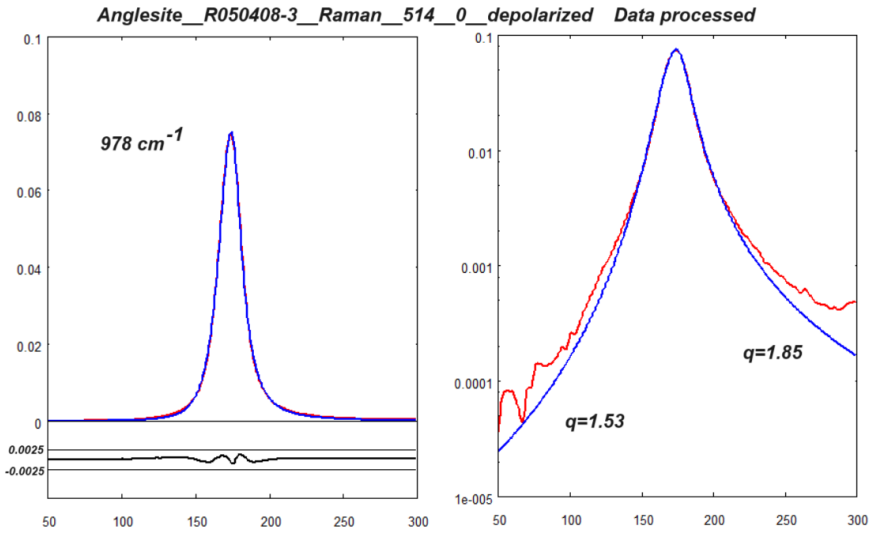

Fig.13: Best fit (blue) onto Anglesite Raman spectrum (red). An asymmetric q-Gaussian is used. The fitting calculation is obtained by minimizing the sum of the squares of the deviations (sum from n501 to n=300 equal to 2.9 x 10^{-5}). The misfit band is 0.005 large.

Calcite

Let us pass to consider Calcite from RRUFF database, https://rruff.info/Calcite/R040170.

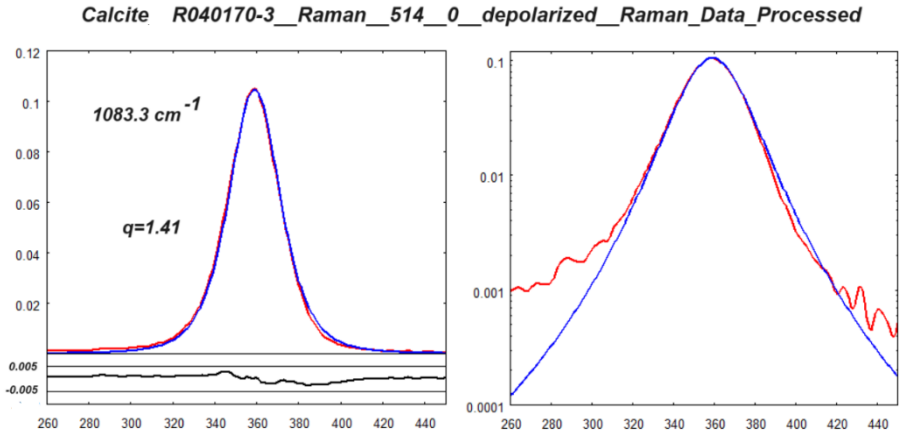

Fig.14: Best fit (blue) onto RRUFF ID R040170 Raman spectrum (red), when a q-Gaussian is used. In the lower part of the figure on the left, the misfit is given. The minimized sum of the squares of the deviations is equal to 3.5 x 10^{-4} (sums from 260 to 450).

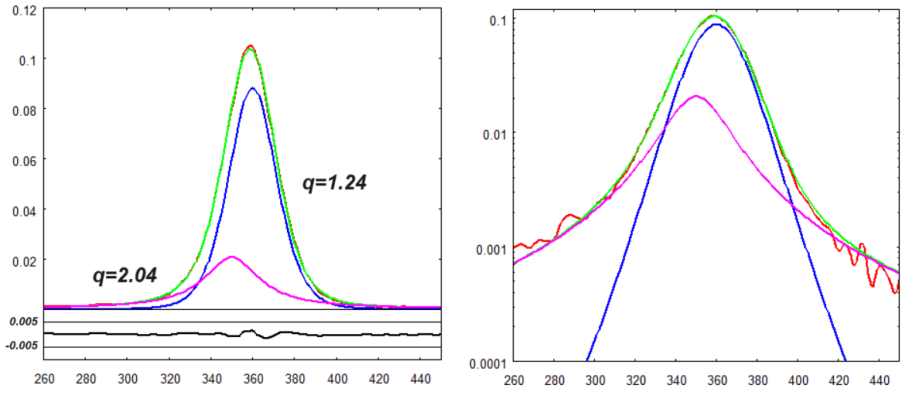

Fig.15: Best fit (green) onto RRUFF ID R040170 Raman spectrum (red), when two q-Gaussians are used. In the lower part of the figure on the left, the misfit is given. The minimized sum of the squares of the deviations is equal to 6.2 x 10^{-5} (sum from 260 to 450).

The band is asymmetric and, to improve the fit with the generalized pseudo-Voigtian made by two q-Gaussians, we need to use different centers of components (see Fig.15). In the following figure, the asymmetric q-Gaussian is involved (the center is the same as in the Fig.14).

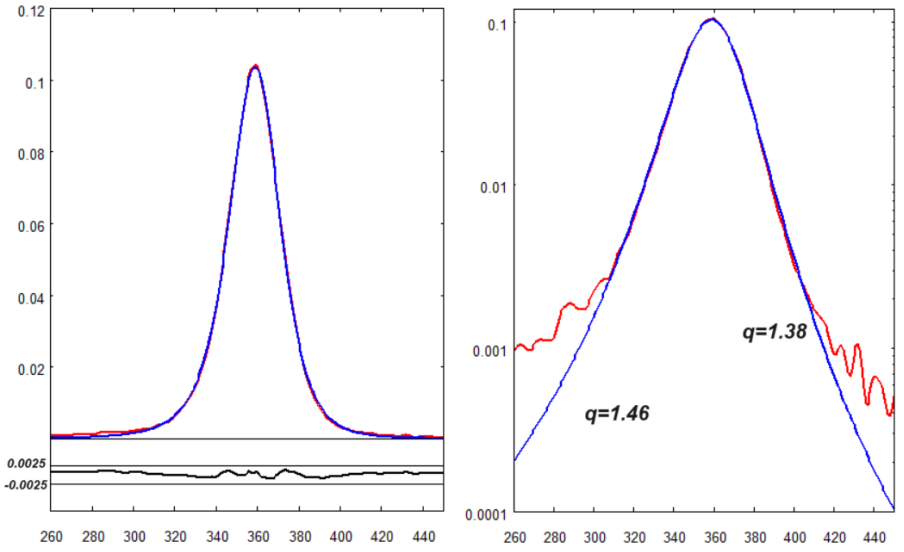

Fig.16: Best fit (blue) onto RRUFF ID R040170 Raman spectrum (red), when an asymmetric q-Gaussian is used. In the lower part of the figure on the left, the misfit is given. The minimized sum of the squares of the deviations is equal to 1.2 x 10^{-4} (sum from 260 to 450).

Manganite

From RRUFF archive let us consider https://rruff.info/Manganite/R060827 (unoriented, 532 nm).

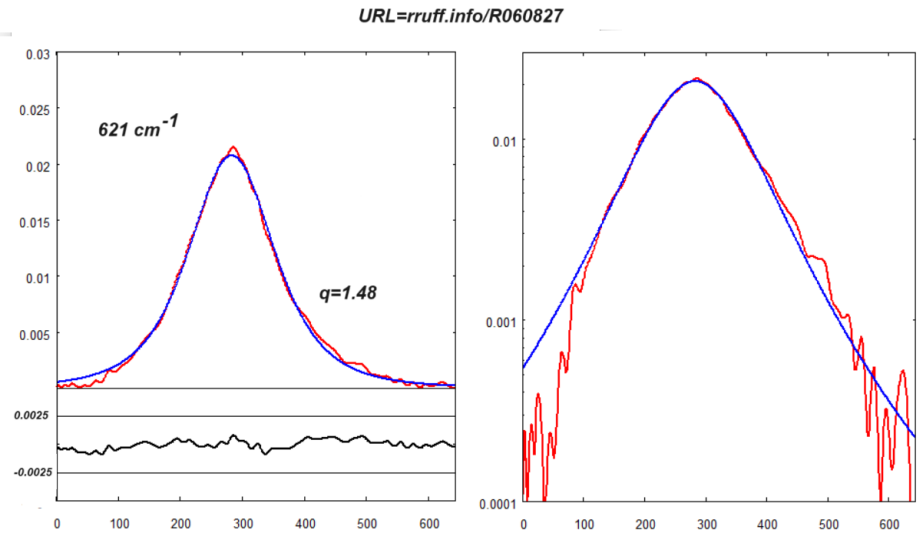

Fig.17: Best fit (blue) onto RRUFF ID R060827 Raman spectrum (red), when a q-Gaussian is used. In the lower part of the figure on the left, the misfit is given. The minimized sum of the squares of the deviations is equal to 1.0 x 10^{-4} (sums from 1 to 630).

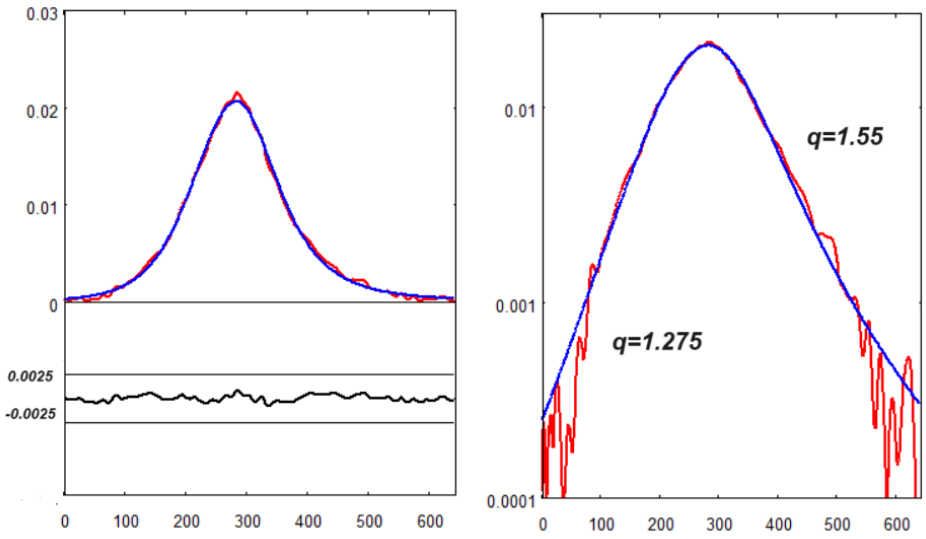

Fig.18: Best fit (blue) onto RRUFF ID R060827 Raman spectrum (red), when an asymmetric q-Gaussian is used. In the lower part of the figure on the left, the misfit is given. The minimized sum of the squares of the deviations is equal to 6.1 x 10^{-5} (sum from 1 to 630).

Asymmetry is evident, so the use of a q-generalized pseudo-Voigtian function is not considered.

Phlogopite

https://rruff.info/Phlogopite/R040144

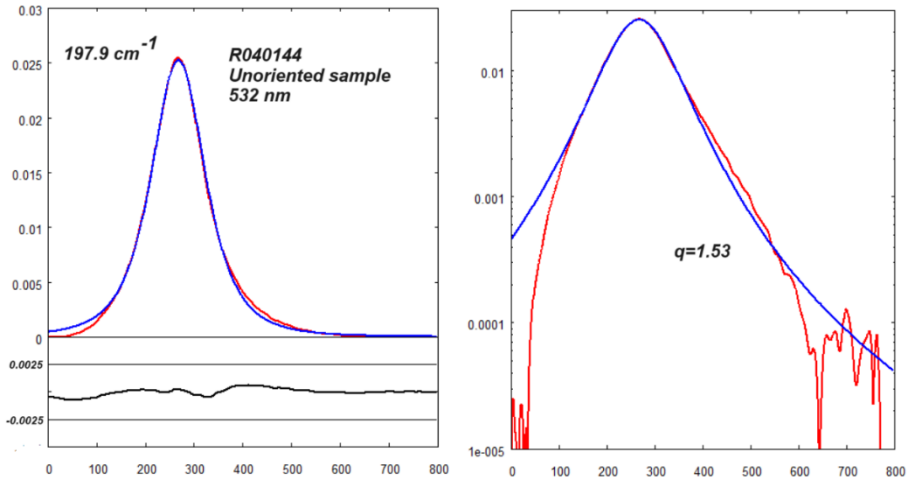

Fig.19: Best fit (blue) onto RRUFF ID R040144 Raman spectrum (red), when a q-Gaussian is used. In the lower part of the figure on the left, the misfit is given. The minimized sum of the squares of the deviations is equal to 8.1 x 10^{-5} (sums from 1 to 800).

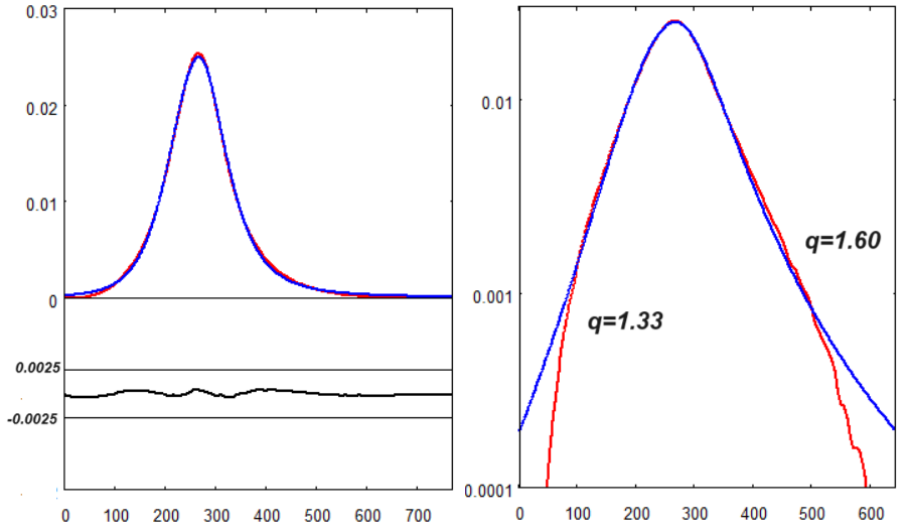

Fig.20: Best fit (blue) onto RRUFF ID R040144 Raman spectrum (red), when an asymmetric q-Gaussian is used. In the lower part of the figure on the left, the misfit is given. The minimized sum of the squares of the deviations is equal to 4.2 x 10^{-5} (sum from 1 to 800).

Spherocobaltite

https://rruff.info/spherocobaltite/display=default/R060497

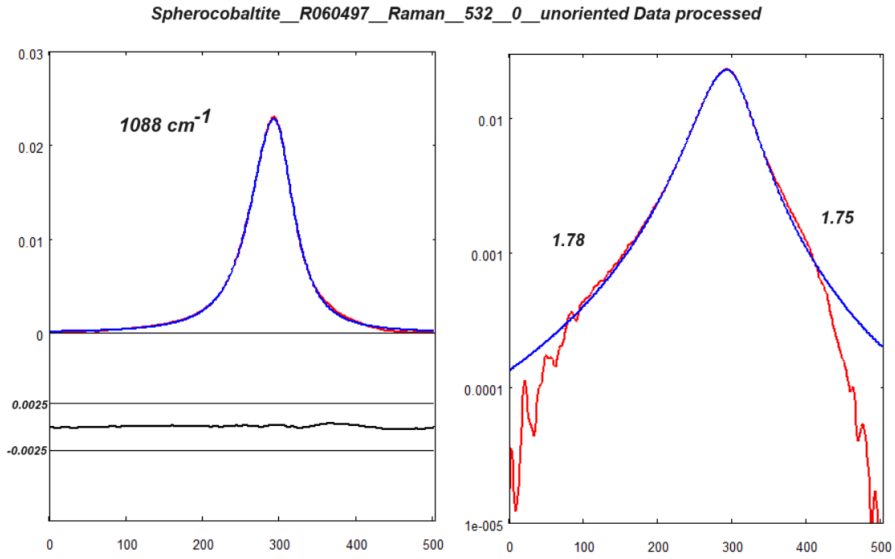

Fig.21: Best fit (blue) onto RRUFF ID R040144 Raman spectrum (red), when an asymmetric q-Gaussian is used. In the lower part of the figure on the left, the misfit is given. The minimized sum of the squares of the deviations is equal to 9.6 x 10^{-6} (sum from 1 to 500).

Just in one of the proposed cases, Fig.15, we needed Lorentzian wings. And this is a case which is clearly asymmetric. In all the other plots, the asymptotic behavior is described by a q parameter lower than 2. The asymptotic Lorentzian term a/x^2 is replaced by $a/[(q-1)x^2]^{1/(q-1)}$. The conclusion is that we need the q-Gaussians for fitting Raman bands.

Appendix A

As previously told, Moyano et al., 2006, are indicating that the q-Gaussian "recovers the t-Student distribution with *l* degrees of freedom if q = (3 + *l*)/(*1* + l). For *l* = 1, hence q = 2, we get the Cauchy-Lorentz distribution". Let us evaluate q as a function of the degrees of freedom (integer values) (see the Fig.A1). Using integers for the degree-of-freedom, the q-parameter has discrete values. This fact tells us that the q-Gaussian is not the t-Student function. If we imagine building a fitting approach of spectra based on integers, we have not the possibility of using the q-Gaussian with q- parameter between 2 and 5/3, for instance. And in all the fitting experiments on Raman data that we did, the use of a real q parameter is fundamental. Moreover, from the point of view of the numerical approach, the use of a parameter in the range from 1 to 2, or even from 1 to 3, is clearly convenient. If we would like to use the t-Student parametrization, the range is from 1 to infinity, besides being the parameter considered as real and not as an integer.

In Wikipedia: t-Student = $C\left[1+\frac{1}{\nu^2}(x-x_o)^2\right]^{-(\nu+1)/2}$

Then $\nu=\frac{3-q}{q-1}$, and here we can see that q must be less than 3. If q=1.8, for instance, then $\nu=1.5$.

The t-Student and the q-Gaussian functions are considered to form two different families by Nielsen and Okanura, 2022. "The Cauchy [Lorentzian] distributions belong to two larger families of distributions: Namely, the t-Student distributions (for ν=1 degrees of freedom) and the q-normal distributions [Naudts] (for q=2). … In information theory, the Cauchy distributions have been used to model and analyze severe non-Gaussian noise with infinite variance … modeling so-called Cauchy channels" (Nielsen & Okamura, 2022, and references therein). "Cauchy distributions are t-Student distributions with one degree of freedom and thus have heavier tails than Gaussian distributions which make them attractive for analyzing a variety of stochastic phenomena in source/channel coding and quantization" (Nielsen & Okamura mentioning Farvardin & Modestino).

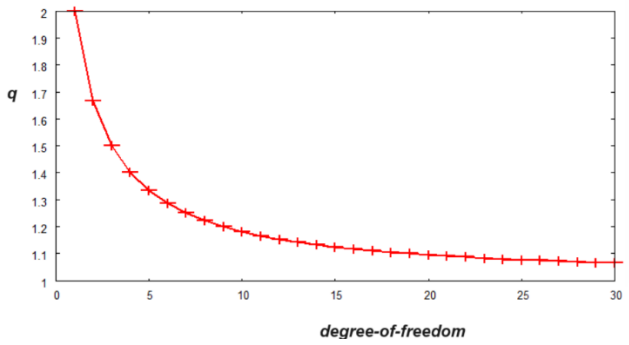

Fig. A1

References

1. Band, Y. B. (2006). Light and Matter: Electromagnetism, Optics, Spectroscopy and Lasers. ISBN: 978-0-471-89931-0 September 2006 656 Pages
2. Cope, D., & Lovett, R. J. (1987). A general expression for the Voigt profile. Journal of Quantitative Spectroscopy and Radiative Transfer, 37(4), 377-389.
3. Devi, S. (2021). Asymmetric Tsallis distributions for modeling financial market dynamics. Physica A: Statistical Mechanics and Its Applications, 578, 126109
4. Farvardin, N., & Modestino, J. W. (1984). Optimum quantizer performance for a class of non-Gaussian memoryless sources, IEEE Trans. Inf. Theory, vol. IT-30, no. 3, pp. 485-497, May 1984.
5. Hanel, R., Thurner, S., & Tsallis, C. (2009). Limit distributions of scale-invariant probabilistic models of correlated random variables with the q-Gaussian as an explicit example. The European Physical Journal B, 72(2), 263.
6. Hanor, J. (2000). Barite-celestine geochemistry and environments of formation. Reviews in Mineralogy. Washington, DC: Mineralogical Society of America. 40(1), 193–275. doi:10.2138/rmg.2000.40.4. ISBN 0-939950-52-9.
7. Kirillov, S. A. (2004). Novel approaches in spectroscopy of interparticle interactions. Raman line profiles and dynamics in liquids and glasses. Journal of molecular liquids, 110(1-3), 99-103.
8. Kirillov, S. (2004). Novel approaches in spectroscopy of interparticle interactions. Vibrational line profiles and anomalous non-coincidence effects. In Novel Approaches to the Structure and

Dynamics of Liquids: Experiments, Theories and Simulations; Springer: Berlin/Heidelberg, Germany, 2004; pp. 193–227
9. Kruschke, J. K. (2015). Doing Bayesian Data Analysis (2nd ed.). Academic Press. ISBN 9780124058880. OCLC 959632184.
10. Lafuente, B., Downs, R. T., Yang, H., & Stone, N. (2015). 1. The power of databases: The RRUFF project. In Highlights in mineralogical crystallography (pp. 1-30). De Gruyter (O).
11. Meier, R. J. (2005). On art and science in curve-fitting vibrational spectra. Vibrational spectroscopy, 2(39), 266-269.
12. Merlen, A., Buijnsters, J. G., & Pardanaud, C. (2017). A guide to and review of the use of multiwavelength Raman spectroscopy for characterizing defective aromatic carbon solids: From graphene to amorphous carbons. Coatings, 7(10), 153.
13. Moyano, L. G., Tsallis, C., & Gell-Mann, M. (2006). Numerical indications of a q-generalised central limit theorem. Europhysics Letters, 73(6), 813.
14. Naudts, J. (2009). The q-exponential family in statistical physics. Central European Journal of Physics, 7, 405-413.
15. Nielsen, F., & Okamura, K. (2022). On f-divergences between Cauchy distributions. IEEE Transactions on Information Theory, 69(5), 3150-3171.
16. Rautian, S. G. (1958). Real spectral apparatus. Soviet Physics Uspekhi, 1(2), 245.
17. Ross, K. (2022). An Introduction to Bayesian Reasoning and Methods. 2022-03-04. https://bookdown.org/kevin_davisross/bayesian-reasoning-and-methods/
18. Seshadri, K., & Jones, R. N. (1963). The shapes and intensities of infrared absorption bands—A review. Spectrochimica Acta, 19(6), 1013-1085
19. Tatum, J. (2022). Combination of Profiles. (2022, March 5). University of Victoria. https://phys.libretexts.org/@go/page/6710
20. Sparavigna, A. C. (2022). Entropies and Logarithms. Zenodo. DOI 10.5281/zenodo.7007520
21. Sparavigna, A. C. (2023). q-Gaussian Tsallis Line Shapes and Raman Spectral Bands. International Journal of Sciences, 12(03), 27-40. http://dx.doi.org/10.18483/ijSci.2671
22. Sparavigna, A. C. (2023). q-Gaussian Tsallis Functions and Egelstaff-Schofield Spectral Line Shapes. International Journal of Sciences, 12(03), 47-50. http://dx.doi.org/10.18483/ijSci.2673
23. Sparavigna, A. C. (2023). q-Gaussian Tsallis Line Shapes for Raman Spectroscopy (June 7, 2023). SSRN Electronic Journal. http://dx.doi.org/10.2139/ssrn.4445044
24. Sparavigna, A. C. (2023). Formamide Raman Spectrum and q-Gaussian Tsallis Lines (June 12, 2023). SSRN Electronic Journal. http://dx.doi.org/10.2139/ssrn.4451881
25. Sparavigna, A. C. (2023). Tsallis and Kaniadakis Gaussian functions, applied to the analysis of Diamond Raman spectrum, and compared with Pseudo-Voigt functions. Zenodo. https://doi.org/10.5281/zenodo.8087464
26. Sparavigna A. C. (2023). Tsallis q-Gaussian function as fitting lineshape for Graphite Raman bands. ChemRxiv. Cambridge: Cambridge Open Engage; 2023.
27. Sparavigna A. C. (2003). Fitting q-Gaussians onto Anatase TiO2 Raman Bands. ChemRxiv. Cambridge: Cambridge Open Engage; 2023.
28. Sparavigna, A. C. (2023). Q-Gaussians and the SERS Spectral Bands of L-Cysteine and Cysteamine. ChemRxiv. doi:10.26434/chemrxiv-2023-9swp9-v2
29. Sparavigna, A. C. (2023). SERS Spectral Bands of L-Cysteine, Cysteamine and Homocysteine Fitted by Tsallis q-Gaussian Functions. International Journal of Sciences, 12(09), 14–24. https://doi.org/10.18483/ijsci.2721
30. Sparavigna, A. C. (2023). Asymmetric q-Gaussian functions to fit the Raman LO mode band in Silicon Carbide. ChemRxiv. Cambridge Open Engage; 2023.
31. Svelto, O. (1970). Principi dei laser. Tamburini editore.
32. Townsend, R. (2008). Astronomy 310, Stellar Astrophysics, Fall Semester 2008, Lecture Notes, https://web.archive.org/web/20230421054452/http://user.astro.wisc.edu/~townsend/resource/teaching/astro-310-F08/17-line-profiles-2.pd

33. Tsallis, C. (1988). Possible generalization of Boltzmann-Gibbs statistics. Journal of statistical physics, 52, 479-487.
34. Tsallis, C. (1995). Some comments on Boltzmann-Gibbs statistical mechanics. Chaos, Solitons & Fractals, 6, 539-559.
35. Umarov, S., Tsallis, C., Steinberg, S. (2008). On a q-Central Limit Theorem Consistent with Nonextensive Statistical Mechanics. Milan J. Math. Birkhauser Verlag. 76: 307–328. doi:10.1007/s00032-008-0087-y. S2CID 55967725.